applied sciences

MDPI

Article

Design of an Active and Passive Control System of Hand Exoskeleton for Rehabilitation

Fuhai Zhang *, Legeng Lin, Lei Yang and Yili Fu *

State Key Laboratory of Robotics and System, Harbin Institute of Technology, Harbin 150001, China; vaegreen@outlook.com (L.L.); yangleihit@163.com (L.Y.)

* Correspondence: zfhhit@hit.edu.cn (F.Z.); meylfu@163.com (Y.F.); Tel.: +86-0451-8640-3219 (F.Z.)

Received: 30 April 2019; Accepted: 29 May 2019; Published: 3 June 2019

Abstract: Aiming at stroke patients' hand rehabilitation training, we present a hand exoskeleton with both active and passive control modes for neural rehabilitation. The exoskeleton control system is designed as a human–robot interaction control system based on field-programmable gate array (FPGA) and Android mobile terminal with good portability and openness. Passive rehabilitation pattern based on proportional derivative (PD) inverse dynamic control method and active rehabilitation pattern based on impedance method, are established respectively. By the comparison of the threshold value and the force on the fingertip of the exoskeleton from the sensor, the automatic switch between active and passive rehabilitation mode is accomplished. The hand model is built in Android environment that can synchronize the movement of the hand. It can also induce patients to participate in rehabilitation training actively. To verify the proposed control approach, we set up and conduct an experiment to do the passive rehabilitation mode, active rehabilitation mode, and active plus passive mode experimental researches. The experiment results effectively verify the feasibility of the exoskeleton system fulfilling the proposed control strategy.

Keywords: rehabilitation; hand exoskeleton; control system; mode switch

1. Introduction

Stroke often results in a combination of cognitive, sensory, and motor impairments. Now, it has become one of the main diseases threatening human survival and health [1,2]. The most common impairment of stroke is hemiparesis, which results in dyskinesia of some parts of the body. It reflects not only in the upper and lower limbs, but also in the loss of motor function of the hand [2]. It was verified by rehabilitation medicine that exercises with high strength and repeatability can stimulate cortical layer to recombine to help the stroke patients learn to control the motion again [3]. The application of robotics and related technologies has greatly promoted the development of clinical techniques [4–6]. Recent researches have shown that exoskeleton devices are feasible and effective for hand rehabilitation [7,8].

Hand is one of the most important limbs of humans, and the rehabilitation of hand motor function can be assisted by exoskeleton robots [9–11]. Many dexterous and advanced mechanisms of hand exoskeletons have been studied and developed. But not all of them are developed for hand rehabilitation. For example, some of them are designed for master–slave systems [12,13] and some others are designed as force-feedback devices [14]. They are limited in the number of independently actuated degrees of freedom. Their mechanism design ideas can be used as a reference for the study of the hand rehabilitation exoskeleton [15–19]. However, due to the special rehabilitation application, we need to modify the mechanism to make sure that exoskeleton and each finger joint have the same center of rotation, which avoids secondary injuries when the exoskeleton has direct contact with the hand [20].

Control system and methods study of the exoskeleton manipulator are also important research categories. The most popular control system of rehabilitation training is a closed loop control system with sensors [20], such as force sensors [21,22] and electromyography (EMG) sensors [23]. The most commonly reported rehabilitation modes provided by developed rehabilitation exoskeletons are the continuous passive motion (CPM) and the active assisted movement (AAM). Some exoskeleton systems are designed for passive rehabilitation mode based on CPM [24]. The passive mode is useful for preventing muscle contractures in early rehabilitation stage. But its effectiveness in the mid-to-late stage is limited when patients can initiate movement but have difficulty in completing it. Some other exoskeleton systems are designed for active rehabilitation control mode based on AAM [25]. The active mode could make up the shortcomings of passive mode in mid-to-late rehabilitation stage. Nowadays, most systems have only one of the modes mentioned above, which is not suitable for the whole scale of rehabilitation, especially the middle rehabilitation stage when patients have some residual motion capability but have not yet reached the normal level. Therefore, if there were two kinds of rehabilitation modes that could switch actively according to patients' rehabilitation status, it can promote hand rehabilitation more effectively.

In addition, the rehabilitation exercises in a virtual environment will be more interesting. It will induce the patients to take the exercise more actively [26,27]. The patients will be more desired to take the exercise so the effect of rehabilitation will be better, such as Hand Mentor Pro^{TM} (Motus Nova, Atlanta, GA, USA) [28]. But because the rehabilitation interface of this kind of device mainly adopts hardware system based on PC or dedicated closed hardware system, it is too expensive, not open and not portable [29].

In this paper, a new kind of hand exoskeleton system has been introduced. The introduced mechanism can adapt to fingers with different thicknesses and lengths and prevent the secondary injuries. Hardware system and human–robot interactive rehabilitation software based on Android system are also designed. The method for passive rehabilitation based on proportional derivative (PD) inverse dynamic control and the method for active rehabilitation based on impedance control are established respectively. Two kinds of rehabilitation modes could switch actively according to contact forces between fingers and exoskeleton in different rehabilitation stages. Finally, the feasibility of the control system and the control strategy has been verified through the experiments.

2. Exoskeleton Mechanism Description

2.1. Overall Design

The design of the exoskeleton mechanism has the following characteristics. Adopting proposed circuitous joints composed of the symmetric pinion and rack mechanism (SPRM) and the parallel sliding mechanism realize the nonlinear stretching displacement of the joint to cover wide workspace of the finger and ensure the force exerted by the exoskeleton is perpendicular to the bone of the finger. The control system on the forearm drives Bowden cable to accomplish the action.

Adopting exoskeleton technology, we design the hand rehabilitation exoskeleton as a wearable glove. The joint mechanisms and the number of degrees of freedom (DOF) are designed according to the physiological structure of the fingers, as shown in Figure 1. The overall mechanical system is composed of three parts, that is, the exoskeleton finger mechanism, the adaptive dorsal metacarpal base, and the Bowden cable driven actuator. The exoskeleton, which is compact and portable, can fulfill rehabilitation training for all the joints of the fingers. Every exoskeleton finger has four rotational DOFs. The rear-mounted driven actuator module can be placed on the forearm of the patient, connecting the hand exoskeleton by Bowden cable, which is portable and can relieve the burden from the patient's wrist and fingers.

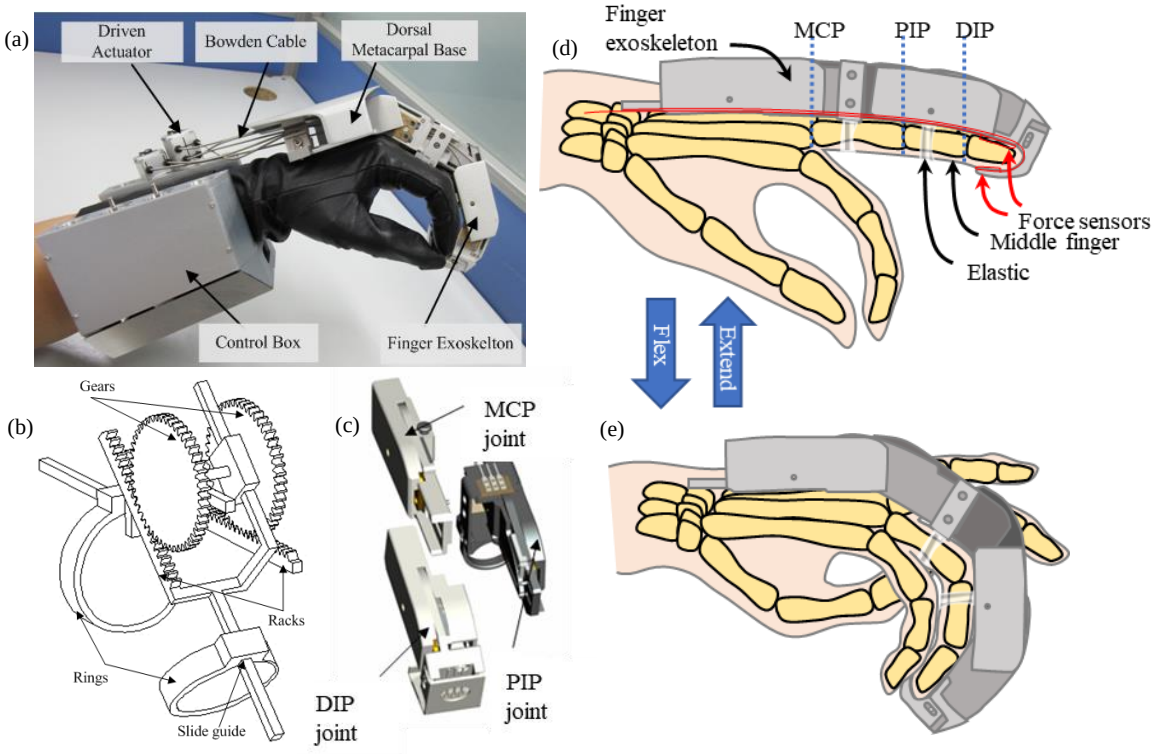

Figure 1. A hand exoskeleton system for rehabilitation: (**a**) overview; (**b**) the symmetric pinion and rack mechanism (SPRM) with the parallel mechanism; (**c**) the three joint modules; (**d**) the exoskeleton is attached to the extended middle finger by elastics and the exoskeleton is on the beginning state; (**e**) the middle finger with the exoskeleton flexes to the max range.

2.2. Joint Design

The key problem of the hand exoskeleton design is the design of the joints. The exoskeleton adopts the SPRM with the parallel mechanism as the joint module, which includes the metacarpophalangeal (MCP) joint, the proximal interphalangeal (PIP) joint, and the distal interphalangeal (DIP) joint, as shown in Figure 1b,c. The mechanism has the advantages of the SPRM and the parallel mechanism, which can realize the telecentric motion around the joint center and adapt to fingers of different thicknesses. Meanwhile, by adjusting the lengths between the exoskeleton joints, the exoskeleton can also adapt to fingers of different lengths. In addition, the force exerted by the exoskeleton is perpendicular to the finger bones, which avoids secondary damage [30].

3. Design of Hardware and Software

3.1. Control System Architecture

The control system of the hand rehabilitation exoskeleton is composed of the hardware system, the mechanical system, and the human–robot interface rehabilitation software, as shown in Figure 2a. The control system adopts hierarchical control strategy, the upper layer control and the interface are designed on the tablet based on Android, and the lower layer control and the data collection are designed on the system on programmable chip (SOPC) based on field-programmable gate array (FPGA) chip. Nios II soft core is embedded into the SOPC as the core processor. The lower layer control algorithm is integrated on the Nios II, which can accomplish high-intensity data collection, calculation, and real-time control. The lower layer hardware and the upper layer interface software are connected by Bluetooth communication module.

The basic working principle is as follows: the hand rehabilitation exoskeleton is worn on the patient's hand whose motion status is detected by the force sensors and angle sensors. The force

sensors can detect the forces exerted on the exoskeleton tips in real time. The angle sensors send the data of exoskeleton displacement to the Micro-Controller Operating Systems II (MicroC/OS-II, stylized as μC/OS-II) system, which provides the control of exoskeleton with status parameters. The control system sends the displacement information of exoskeleton joints to the Android system by Bluetooth communication module in order to actuate the motion of the finger model in a virtual environment.

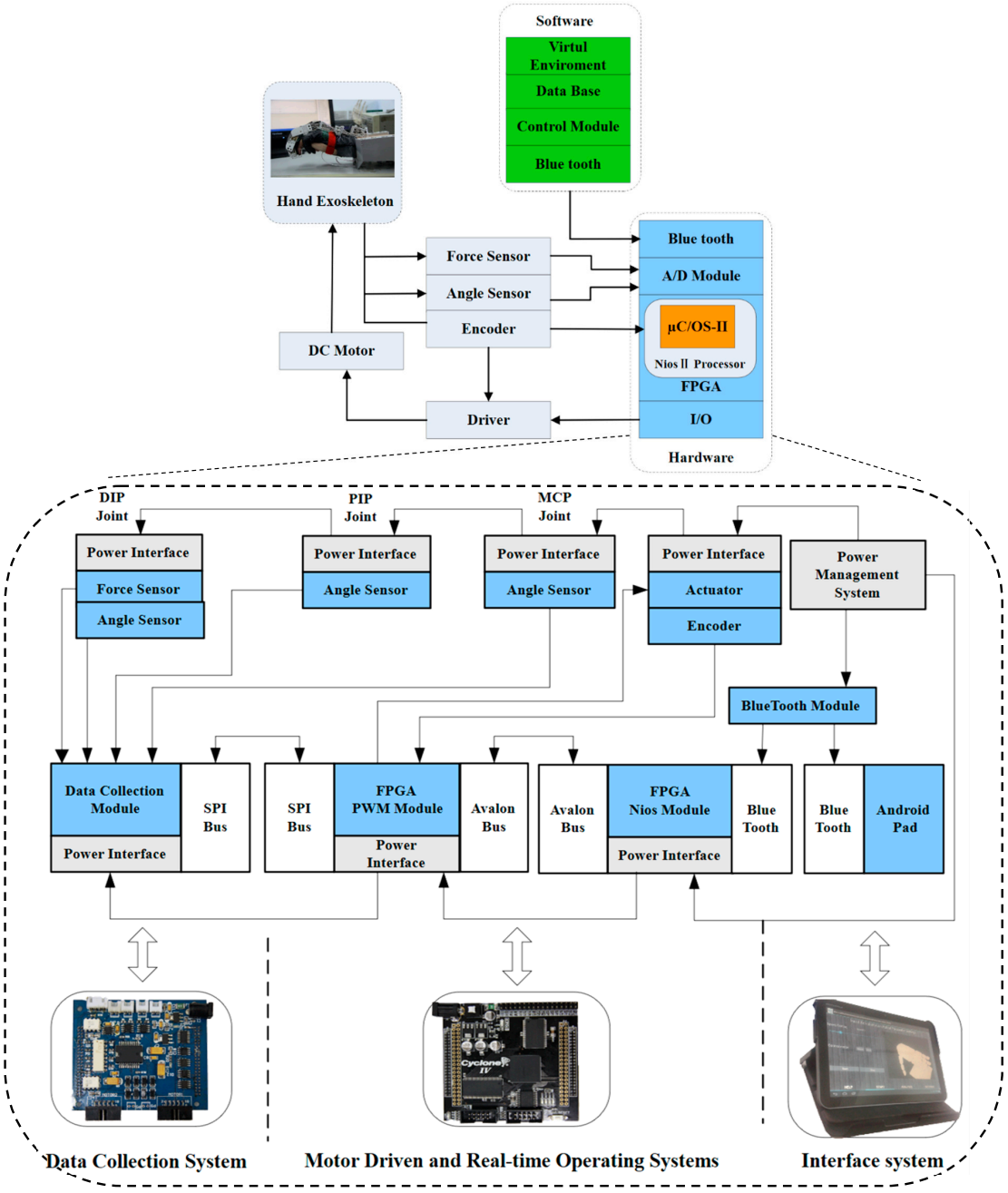

Figure 2. (**a**) Control system layout; (**b**) the control hardware composition.

3.2. Control Hardware

The hardware composition and relationship are shown in Figure 2b. The hardware system can accomplish data collection of the sensors and handle the motion parameters of the fingers in real time, and meanwhile, it can satisfy the requirements of high integration level, low power consumption, and portability. The lower layer control system based on FPGA chips can be divided into five subsystems

according to the functions: the real-time task processor module based on Nios II soft core, the DC motor actuator module, the sensor and data collection module, the power management module, and the Bluetooth communication module. By embedding Nios II soft core to the SOPC, the high-intensity calculation and real-time control on the lower layer are integrated into the Nios II soft core. The pulse width modulation (PWM) motor actuator communicates with other modules by the Avalon bus in FPGA, using the motor actuating chip to actuate the motion of DC motor. The data collection module communicates with FPGA by serial peripheral interface (SPI) bus. The signals collected are input into the control system by AD converter in order to sample the torque and joint displacement signals. The encoder signal is sent to the soft core by high-speed optocoupler through quadruplicated frequency and direction judgment circuit to get the motion parameters of the motors. The power management module supplies stable voltages for different modules in the hardware system. The Bluetooth module can communicate with the interface rehabilitation software and transmit parameters bidirectionally.

3.3. Software Interface

The interface based on Android system takes advantage of the portability of mobile devices, which can help the patients get rid of the limitation of fixed occasions and do the rehabilitation training anywhere and anytime. The human–robot interaction rehabilitation software of the hand rehabilitation exoskeleton is developed based on Android 4.0 SDK and supports most of the smartphones and tablets with Android system. The rehabilitation software is composed of the interface layer, data access layer, and virtual reality rehabilitation training layer, as shown in Figure 3.

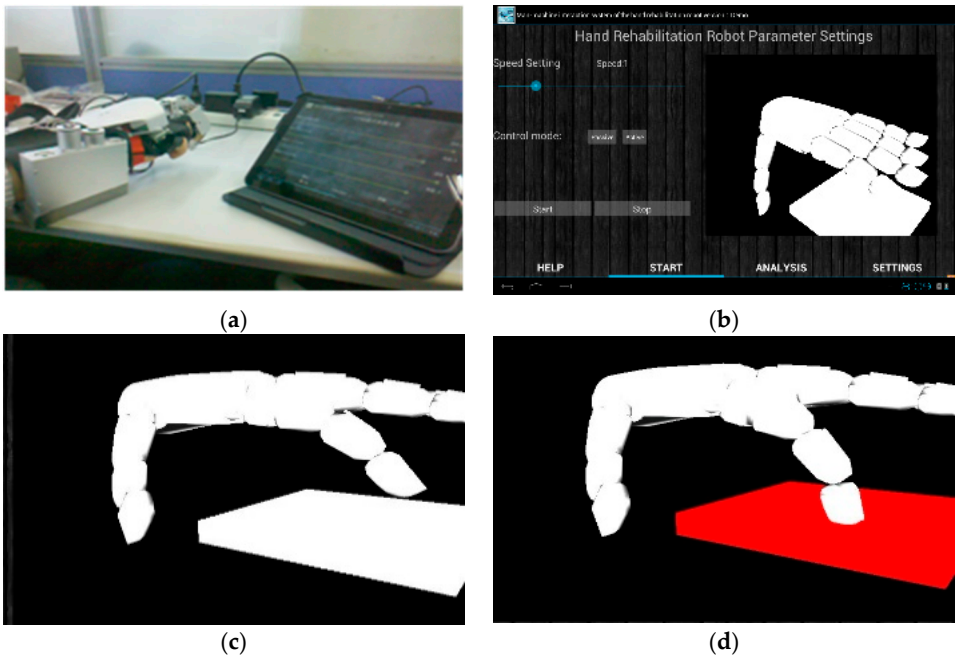

Figure 3. Android software interface: (**a**) whole system; (**b**) interface; (**c**) virtual reality rehabilitation training layer; (**d**) collision detection.

The whole system is shown in Figure 3a. The interface layer is shown in Figure 3b, adopting the tab weight interactive mode to provide doctors or patients with options on rehabilitation modes and control parameters. The data access layer uses the Bluetooth communication module to receive motion parameters of the exoskeleton in real time and store them in the database. The virtual reality rehabilitation training layer receives the motion parameters through the data access to actuate the real-time motion of the virtual model in Android environment, as shown in Figure 3c. In addition, the contact plate is set on the functional position of the exoskeleton motion, and collision detection

between the virtual hand and the contact plate is used to inform the system that the hand has reached the functional position, as shown in Figure 3d.

4. Active and Passive Control

4.1. Control Strategy

The overall control strategy of the hand rehabilitation exoskeleton designed in this paper is shown in Figure 4. If it is detected by the sensors that the patient's hand can do flexion-extension, then the active rehabilitation mode will be adopted, and the exoskeleton will follow the motion of the fingers. Otherwise, the passive rehabilitation mode will be adopted, and the exoskeleton will actuate the fingers to move. The motion ability of the hand is judged by the contact force between the exoskeleton and the hand detected by the force sensors, which is used for the real-time switch of the control strategy between active and passive rehabilitation modes.

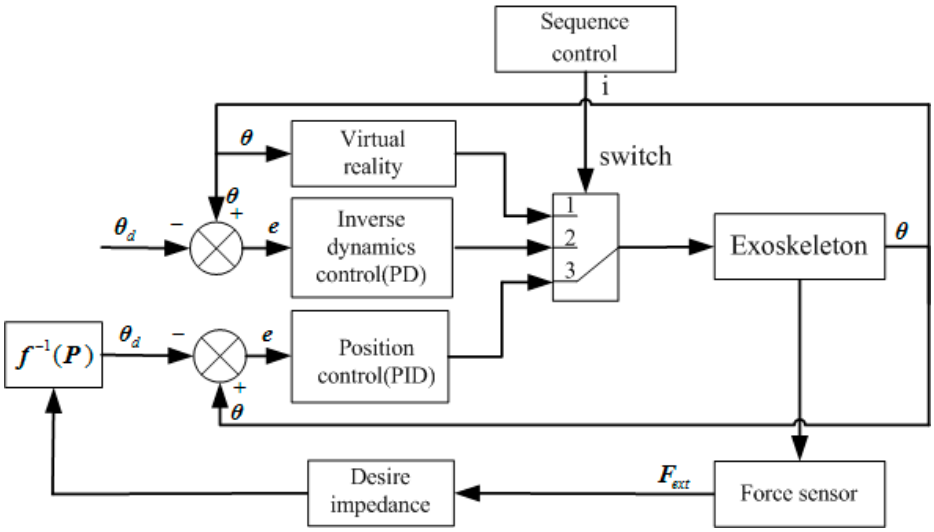

Figure 4. The active/passive control block diagram.

In the passive rehabilitation mode, the control system adopts a highly robust and reliable PD method to control the motion of the patient's finger to the functional position. In this mode, the patient or physician can choose suitable velocity gear for the inverse dynamics control to implement in early rehabilitation stage. Then the exoskeleton helps the finger follow the desired trajectory and move to the functional position at the preset velocity.

In the active rehabilitation mode, the control system adopts impedance control to track the force on the fingertip and track the desired trajectory by the position control loop. In this mode, the patient or physician can preset the resistance according to the patient's movement ability. Then the exoskeleton tries to follow the patient's motion and keep the force between exoskeleton and fingertip around the preset resistance to improve the movement ability.

The active plus passive rehabilitation mode is designed based on the two basic rehabilitation modes, detecting the force between the exoskeleton and the patient's fingertip through the force sensors distributed on the tip. The switch of the two modes is determined by the threshold value. In this mode, if the patient could exert force actively, the control system will switch to the active mode and follow the patient's motion. Otherwise, whenever the patient cannot exert enough force to move the fingers, the control system will switch to the passive mode to help the finger track the desired trajectory to reach the functional position at a preset velocity gear. In order to keep the system stable and compliant, in the control system, the impedance parameter is adjusted to be close to the input velocity parameter in the passive mode to provide smooth rehabilitation experience for the patients.

In the interaction rehabilitation software, when the virtual finger touches the contact plate, the collision signal is sent to the control system that will judge the functional position according to the signal. In the overall rehabilitation control strategy, the switch is accomplished by the sequence controller.

4.2. Modeling

The coordinates of the exoskeleton fingers are shown in Figure 5. Every finger has four joints, which are joint MCP with two DOFs, i.e., yaw (MCP1) and pitch (MCP2), joint PIP and joint DIP. The joint angles of MCP are θ_0, θ_1, the angles of joint PIP and joint DIP are θ_2, θ_3 respectively. The lengths of links are a_0, a_1, a_2, a_3, where $a_0 = 0$.

- Kinematics:

Due to the coupling effect between joint PIP and joint DIP, the ratio is $\theta_2 : \theta_3 = 1 : u$, and MCP1 is an adaptive DOF without actuating. The kinematic relationship between the tip position and the joint angles is:

$$\boldsymbol{P}_t = \begin{bmatrix} x_t \\ y_t \\ z_t \end{bmatrix} = \begin{bmatrix} c\theta_0(a_2c\theta_{12} + a_1c\theta_1 + a_3c\theta_{123}) \\ s\theta_0(a_2c\theta_{12} + a_1c\theta_1 + a_3c\theta_{123}) \\ a_1s\theta_1 + a_2s\theta_{12} + a_3s\theta_{123} \end{bmatrix}, \tag{1}$$

- Dynamics:

The dynamic model of the exoskeleton finger is the foundation of controller design and simulation study. In this paper, the Lagrange method is adopted to build the dynamic model in joint space in order to facilitate the study of the control method. For the exoskeleton model moving in the n-dimensional space, the Lagrange dynamic equation in joint space is:

$$\boldsymbol{D}(\boldsymbol{\theta})\ddot{\boldsymbol{\theta}} + \boldsymbol{h}(\boldsymbol{\theta}, \dot{\boldsymbol{\theta}}) + \boldsymbol{G}(\boldsymbol{\theta}) + \boldsymbol{J}^{\mathrm{T}}\boldsymbol{F}_{ext} = \boldsymbol{\tau}, \tag{2}$$

where $\boldsymbol{D}(\boldsymbol{\theta})$ is the inertia matrix, $\boldsymbol{D}(\boldsymbol{\theta}) \in \boldsymbol{R}^{3\times3}$, $\boldsymbol{h}(\boldsymbol{\theta}, \dot{\boldsymbol{\theta}})$ is the centripetal and Coriolis force, $\boldsymbol{h}(\boldsymbol{\theta}, \dot{\boldsymbol{\theta}}) \in \boldsymbol{R}^{3\times1}$, $\boldsymbol{G}(\boldsymbol{\theta})$ is gravity item, $\boldsymbol{\tau}$ is the joint actuating torque vector, $\boldsymbol{\tau} = \begin{bmatrix} \tau_1 & \tau_2 & \tau_3 \end{bmatrix}^{\mathrm{T}}$, $\boldsymbol{F}_{ext}$ is the force on the exoskeleton fingertip, $\boldsymbol{F}_{ext} = \begin{bmatrix} F_x & F_y & F_z \end{bmatrix}^{\mathrm{T}}$. Considering the coupling effect between joint PIP and joint DIP, i.e., the two SPRM with parallel mechanism are joined together and actuated by the same motor, the motor torque is the sum of the torques of the two coupling joints.

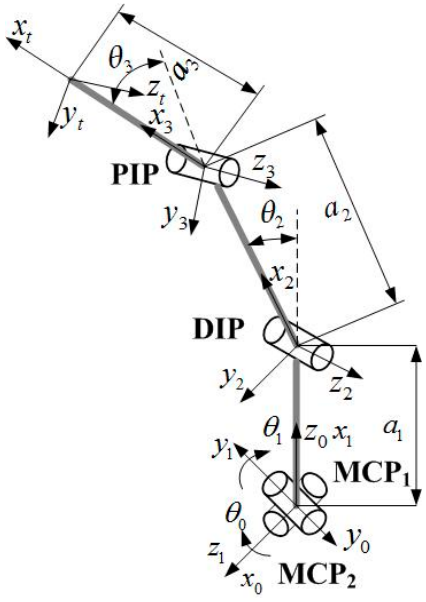

Figure 5. Structure diagram of the single exoskeleton finger.

4.3. Passive Control

Because of the partial or complete loss of motor function, in general, the stroke patients cannot finish the whole rehabilitation training, i.e., they cannot actively control their hands to the functional position. Under this circumstance, the control system of the hand rehabilitation exoskeleton can detect the contact parameters by the force sensors on the fingertips and switch to the passive mode, where the fingers are actuated to the functional position by the exoskeleton. In the passive rehabilitation mode, the goal is to actuate the joints to follow the desired trajectory and move to the preset functional position. The PD control method based on the inverse dynamic compensation is adopted and the control block diagram is shown in Figure 6.

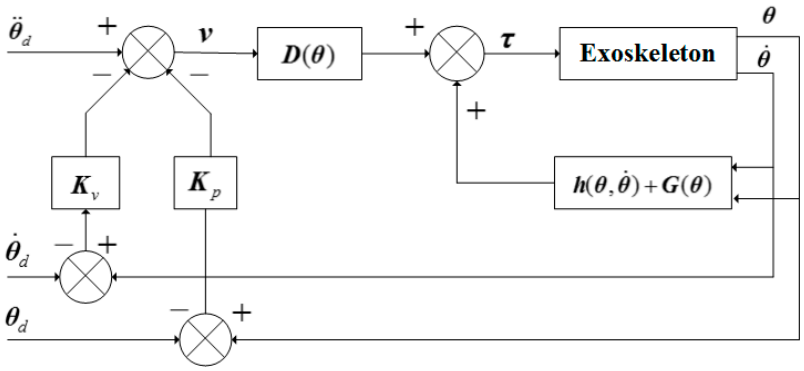

Figure 6. The passive control block diagram.

Defining the trajectory error $\boldsymbol{e}(t) = \boldsymbol{\theta}(t) - \boldsymbol{\theta}_d(t)$ and velocity error $\dot{\boldsymbol{e}}(t) = \dot{\boldsymbol{\theta}}(t) - \dot{\boldsymbol{\theta}}_d(t)$, $\boldsymbol{\theta}_d(t)$ is the desired trajectory of the exoskeleton in joint space, $\boldsymbol{\theta}(t)$ is the actual trajectory in joint space. Assuming the desired trajectory $\boldsymbol{\theta}_d(t), \dot{\boldsymbol{\theta}}_d(t), \ddot{\boldsymbol{\theta}}_d(t)$ are bounded, and by inducing $\boldsymbol{v}$ and substituting it into the dynamic equation in joint space, we have the controller as follows:

$$\boldsymbol{\tau} = \boldsymbol{D}(\boldsymbol{\theta})\boldsymbol{v} + \boldsymbol{h}(\boldsymbol{\theta}, \dot{\boldsymbol{\theta}}) + \boldsymbol{G} \tag{3}$$

substituting Equation (3) into the dynamic equation Equation (2), and we have,

$$\boldsymbol{D}(\ddot{\boldsymbol{\theta}} - \boldsymbol{v}) = \boldsymbol{0}. \tag{4}$$

if $\boldsymbol{D}$ is invertible, then from (4) we have:

$$\ddot{\boldsymbol{\theta}} = \boldsymbol{v}. \tag{5}$$

setting $\boldsymbol{v}$ as the following equation:

$$\boldsymbol{v} = \ddot{\boldsymbol{\theta}}_d - \boldsymbol{K}(\boldsymbol{p})\boldsymbol{e}. \tag{6}$$

substituting (5) into (6), the error equation of the system can be obtained as follows:

$$(\boldsymbol{p}^2\boldsymbol{I} + \boldsymbol{K}(\boldsymbol{p}))\boldsymbol{e} = 0. \tag{7}$$

introducing the PD control method into (7):

$$\boldsymbol{K}(\boldsymbol{p}) = \boldsymbol{K}_v\boldsymbol{p} + \boldsymbol{K}_p, \tag{8}$$

where $\boldsymbol{K}_v$ and $\boldsymbol{K}_p$ are positive diagonal matrices. If we substitute Equations (6) and (8) into Equation (3), the passive rehabilitation control equation can be obtained as:

$$\boldsymbol{\tau} = \boldsymbol{D}(\boldsymbol{\theta})(\ddot{\boldsymbol{\theta}}_d - \boldsymbol{K}_v\dot{\boldsymbol{e}} - \boldsymbol{K}_p\boldsymbol{e}) + \boldsymbol{h}(\boldsymbol{\theta}, \dot{\boldsymbol{\theta}}) + \boldsymbol{G}(\boldsymbol{\theta}). \tag{9}$$

4.4. Active Control

The active rehabilitation mode is that the patients do flexion and extension of the finger actively and the exoskeleton tracks and adapts to the motion status of the patients automatically. The controller does not directly control the exoskeleton to reach the desired configuration, but control it to follow the patient's motion according to the motor ability. According to the impedance model and the input of the force signals on the tips, the trajectory of the exoskeleton finger is planned in real time. The actual motion status parameters are obtained by detecting the output $\boldsymbol{\theta}$ of the exoskeleton, thus we have the control variable $\boldsymbol{e}(t)$. The position controller is used to realize the real-time track of the patient's fingers. The control block diagram is shown in Figure 7.

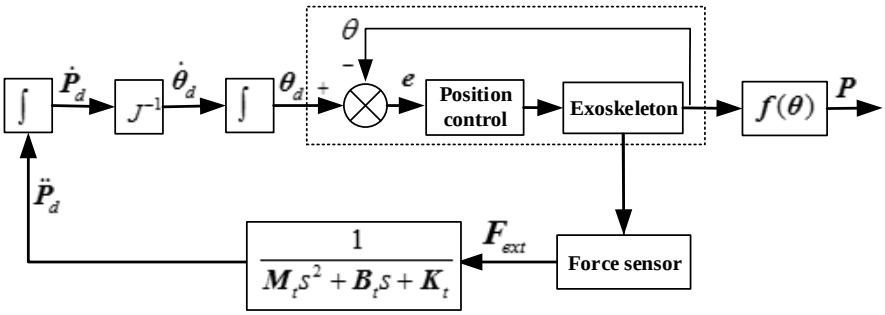

Figure 7. The active control block diagram.

The relationship between the joint space of the exoskeleton and the Cartesian space is

$$\begin{cases} \boldsymbol{P} = \boldsymbol{f}(\boldsymbol{\theta}) \\ \dot{\boldsymbol{P}} = \boldsymbol{J}(\boldsymbol{\theta})\dot{\boldsymbol{\theta}} \end{cases}, \tag{10}$$

where $\boldsymbol{f}(\boldsymbol{\theta})$ is the forward kinematic relationship of the exoskeleton. Taking the derivative of Equation (10) and we have the relationship between the accelerations in joint space and Cartesian space:

$$\ddot{\boldsymbol{P}} = \boldsymbol{J}(\boldsymbol{\theta})\ddot{\boldsymbol{\theta}} + \dot{\boldsymbol{J}}(\boldsymbol{\theta})\dot{\boldsymbol{\theta}}. \tag{11}$$

During the contact of finger and exoskeleton, the relationship between finger and exoskeleton is a second order dynamic relation, and we simplify it as a linear spring model. In Cartesian space, the impedance model is as follows:

$$\boldsymbol{M}_t(\ddot{\boldsymbol{P}} - \ddot{\boldsymbol{P}}_d) + \boldsymbol{B}_t(\dot{\boldsymbol{P}} - \dot{\boldsymbol{P}}_d) + \boldsymbol{K}_t(\boldsymbol{P} - \boldsymbol{P}_d) = \boldsymbol{F}_{ext}, \tag{12}$$

where $\boldsymbol{M}_t$, $\boldsymbol{B}_t$, $\boldsymbol{K}_t$ are objective inertia matrix, objective damping matrix, and objective stiffness matrix, respectively. $\boldsymbol{P}$ and $\boldsymbol{P}_d$ are respectively the actual position and desired position of the exoskeleton fingertip. $\boldsymbol{F}_{ext}$ is the contact force between the finger and the exoskeleton.

Rewriting the impedance model Equation (12) and substituting it into Equations (10) and (11), we have:

$$\ddot{\boldsymbol{\theta}}_d = \ddot{\boldsymbol{\theta}} - \boldsymbol{J}^{-1}\boldsymbol{M}_t{}^{-1}[\boldsymbol{F}_{ext} - \boldsymbol{B}_t(\dot{\boldsymbol{P}} - \dot{\boldsymbol{P}}_d) - \boldsymbol{K}_t(\boldsymbol{P} - \boldsymbol{P}_d)] + \boldsymbol{J}^{-1}\dot{\boldsymbol{J}}\dot{\boldsymbol{\theta}}. \tag{13}$$

Due to the integral of Equation (13) and $\boldsymbol{\theta}_d$ has been obtained, the PID control method is adopted in the position control loop. In the active rehabilitation mode, the position error $\boldsymbol{e}(t)$ is used to make the motor output torque $\boldsymbol{\tau}$ actuate the exoskeleton to follow the desired trajectory, and the relationship between $\boldsymbol{e}(t)$ and $\boldsymbol{\tau}$ is as follows:

$$\boldsymbol{\tau} = \boldsymbol{K}_P \cdot \boldsymbol{e}(t) + \boldsymbol{K}_I \cdot \int_0^t \boldsymbol{e}(t)dt + \boldsymbol{K}_D \cdot \frac{d\boldsymbol{e}(t)}{dt}, \tag{14}$$

where $\boldsymbol{K}_P$, $\boldsymbol{K}_I$, $\boldsymbol{K}_D$ are the proportional, integral, and differential gains of the controller, respectively.

5. Experiments

5.1. Experimental Setup

The experimental setup includes the hand exoskeleton, the hardware of the control system, the Motorola tablet based on Android system, and the 12 V regulated power supply, as shown in Figure 8. A pair of force sensors (Tekscan Company's flexible pressure sensor, 1 lbs) is placed on the top and bottom of the PIP joint of the exoskeleton finger to detect the contact force between the fingertip and the exoskeleton.

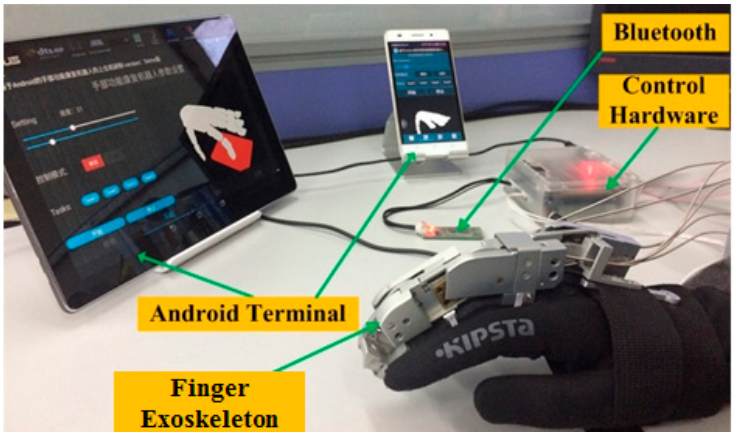

Figure 8. Experimental setup.

The operator can use the tablet to set the start, stop, motion velocity, and contact detection, and send instructions to the exoskeleton by the Bluetooth communication module. Meanwhile, the control system of the exoskeleton detects the motion status of the patient by force sensors in order to decide the rehabilitation mode.

The human–robot interaction rehabilitation software can receive the motion information of the patient's hand in the control system, and the model is shown in the virtual environment in real time to induce the patient to participate in rehabilitation training actively. During the experiment, we choose a healthy human as the rehabilitation subject. The information about the subject's three phalanxes of the middle finger is shown in Table 1. The finger mass is estimated according to the volume [31]. All ethical issues with the study design are in accordance with the local ethical regulations.

Table 1. Finger parameters of subject.

Length of Phalanx (mm)			Weight of Phalanx (g)		
Proximal	**Middle**	**Distal**	**Proximal**	**Middle**	**Distal**
55	34	28	130	65	55

5.2. Experimental Implementation

- Passive rehabilitation mode:

The motion ranges of the joints of the volunteer's middle finger are measured by the NDI Optotrak 3-D measurement system, based on which the desired trajectory of the middle finger in joint space is set as:

$$\boldsymbol{\theta}_d = \begin{pmatrix} -0.10t^3 + 0.50t^2 + 18.50t \\ -0.11t^3 + 0.53t^2 + 19.53t \\ -0.83t^3 + 0.42t^2 + 15.38t \end{pmatrix}. \quad (15)$$

During this experiment, the subject sat before the tablet, wore the glove with exoskeleton on hand, and kept the finger relaxed. The exoskeleton drove the finger to do flexion-extension and track the desired trajectory to make the virtual finger touch the virtual box in the Android tablet. The control block diagram is shown in Figure 6. Control parameters in Equation (9) are $\boldsymbol{K}_v = diag\{0.4, 0.4, 0.4\}$, $\boldsymbol{K}_p = diag\{0.5, 0.5, 0.5\}$. The experiment time was 5 s and the data sampling period was 10 ms.

- Active rehabilitation mode:

The active rehabilitation mode uses impedance algorithm to drive the exoskeleton by the force on the tip collected by the force sensors.

During this experiment, the subject sat before the tablet and wore the glove with exoskeleton on hand. The subject was required to exert force on the finger and keep the finger relaxed alternately to stimulate patients with residual motor ability. In the active rehabilitation mode, the exoskeleton follows the hand. The desired trajectory of the active rehabilitation experiment is from the real-time simulation synchronous with the experiment. Control block diagram of the simulation is shown in Figure 7. The contact force in the control law Equation (14) is from the real-time data obtained from the experiment. Other control parameters in Equation (13) during simulation are $\boldsymbol{M}_t = diag\{100, 100, 100\}$, $\boldsymbol{B}_t = diag\{0.1, 0.1, 0.1\}$, $\boldsymbol{K}_t = diag\{0.2, 0.2, 0.2\}$. The parameters in Equation (14) are chosen as $K_P = 0.5$, $K_I = 0.0625$, $K_D = 0.4$. In the simulation, Equation (2) is adopted as the exoskeleton model, and the dynamic parameters are shown in Table 2. During the experiment, the sampling period is 10 ms, and the motion time is 28 s.

Table 2. Dynamic parameters of the single finger of the exoskeleton.

Link i	m_i (kg)	I_{xx} (kg·mm^2)	I_{yy} (kg·mm^2)	I_{zz} (kg·mm^2)
1	0.048	10.286	31.093	31.720
2	0.029	12.325	37.057	43.224
3	0.037	14.489	32.140	36.589

- Active plus passive rehabilitation mode:

The active plus passive experiment of the hand rehabilitation exoskeleton is the combination of active and passive rehabilitation modes.

During this experiment, the subject sat before the tablet and wore the glove with exoskeleton on hand. The subject was required to exert force on the finger and occasionally relax the finger to stimulate patients with incomplete motor ability. The sampling period was 10 ms, and the motion time was 5 s. The threshold value of the force on the fingertip was preset to switch the mode between the active and passive rehabilitation automatically. In this experiment, the threshold value was set as 0.6 N from pre-experiments. The desired trajectory of the experiment was also obtained by the real-time simulation. Specifically, if $\boldsymbol{F}_{ext} \geq 0.6$ N, then the system considers that the patient is willing to and able to move actively, hence the control system will switch to the active mode. Otherwise, if $\boldsymbol{F}_{ext} < 0.6$ N, then the passive rehabilitation mode is chosen. In order to ensure the stability of the motion, the angular velocities of the joints were calculated by the passive control, and the trajectories were obtained by the integral of velocity.

5.3. Experimental Results

- Passive rehabilitation mode:

From Equation (1) the trajectories of $\boldsymbol{\theta}_d$ and $\boldsymbol{\theta}$ in Cartesian space were calculated by forward kinematics, as shown in Figure 9. The trajectories in x_t direction and y_t direction are shown as the curves in Figure 9a,b respectively, and the mean ± standard deviation of errors are 0.17 ± 0.62 mm and −0.28 ± 0.85 mm, respectively. Therefore, the results show that the motion of the exoskeleton is stable,

and the actual trajectory generally accords with the desired trajectory, tracking the planned trajectory well to do the rehabilitation motion, which can meet the need of passive rehabilitation.

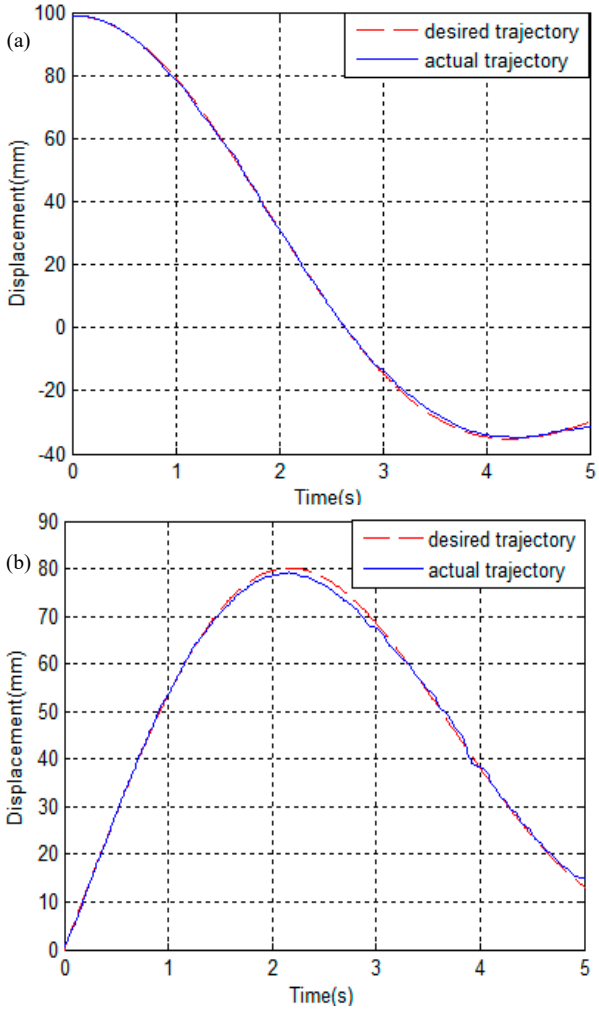

Figure 9. Passive rehabilitation experiment: (**a**) x_t direction displacement; (**b**) y_t direction displacement.

- Active rehabilitation mode:

The real-time simulation results are shown as the desired trajectory (dash lines) in Figure 10a,b. The actual trajectories in x_t direction and y_t direction are shown as the solid line in Figure 10a,b, and the mean ± standard deviation of errors are −0.33 ± 2.04 mm and 0.16 ± 1.92 mm, respectively. The curve of force on the tip collected in the experiment is shown in Figure 10c.

From the figures, when the finger is relaxed, the output of the force sensor on the fingertip of the exoskeleton is close to 0 and the exoskeleton keeps its attitude. When the subject exerts force on the finger, the force sensor can perceive the contact force changes immediately. The exoskeleton can follow the finger motion well to fulfill the control strategy of active rehabilitation mode with resistance at around 3.8 N. The experiment results show that the designed controller has the ability in position tracking and it can automatically track and adapt to the motion status of the patient during active rehabilitation training.

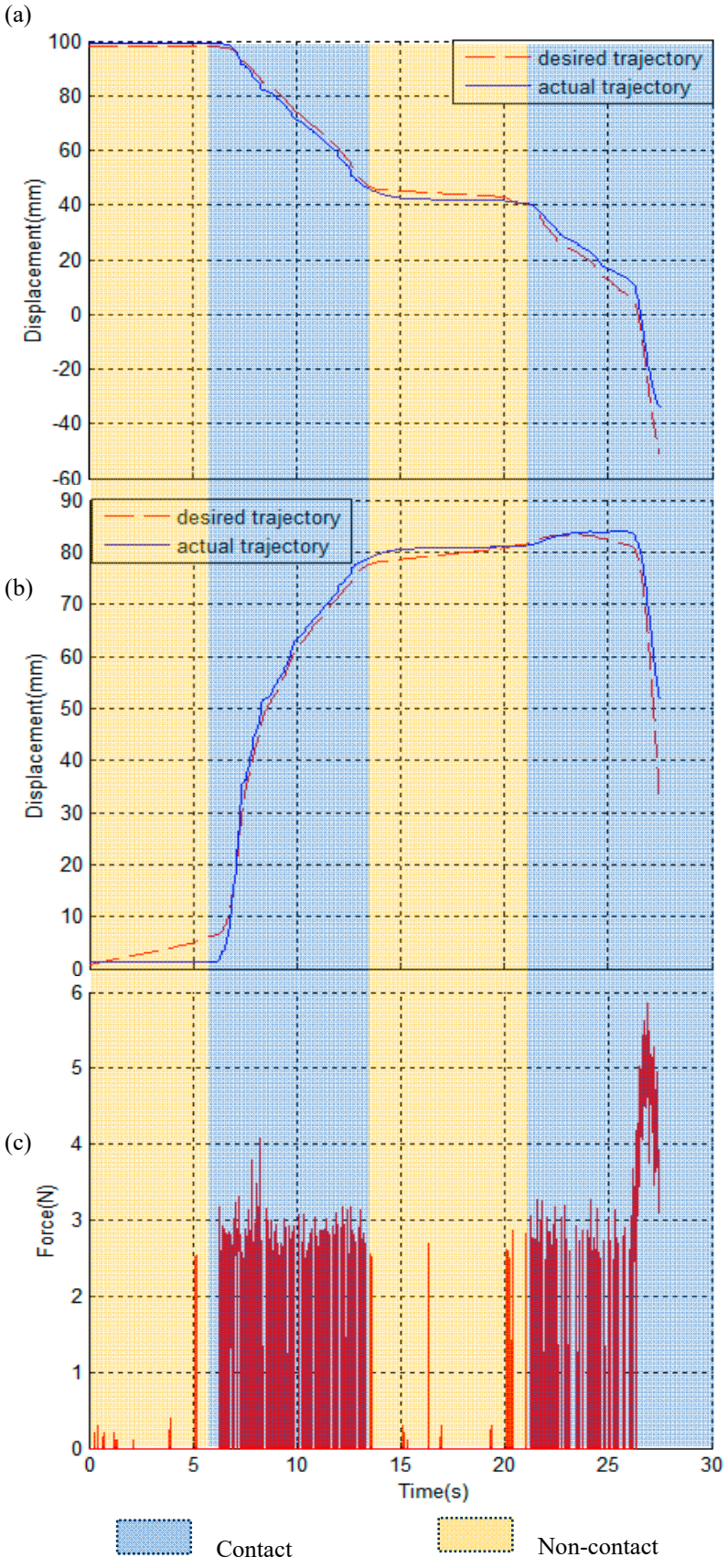

Figure 10. Active rehabilitation experiment: (**a**) x_t direction displacement; (**b**) y_t direction displacement; (**c**) contact force.

- Active plus passive rehabilitation mode:

The dash lines in Figure 11b,d show the desired trajectories of the exoskeleton in x_t and y_t directions, and the mean ± standard deviation of errors are 0.97 ± 1.64 mm and −0.12 ± 1.04 mm, respectively. Figure 11a shows the force on the fingertip collected during the rehabilitation process, and Figure 11b,d shows the actual trajectories of the exoskeleton in x_t and y_t directions.

The hand rehabilitation exoskeleton can judge the rehabilitation intention of the patient by detecting the force on the tip. At about t = 2.4 s, when the subject cannot exert enough force, the force on the tip is smaller than the threshold value. Hence the exoskeleton switches to the passive mode, and the angular velocities are calculated by the passive control, as shown in Figure 11c. At about t = 2.9 s and t = 4 s, when the subject can exert force, the force on the tip of the exoskeleton finger is larger than the threshold value. Hence the exoskeleton is in active rehabilitation mode and follows the subject's motion. The experiment results verify the feasibility of the control strategy and the stability of the system.

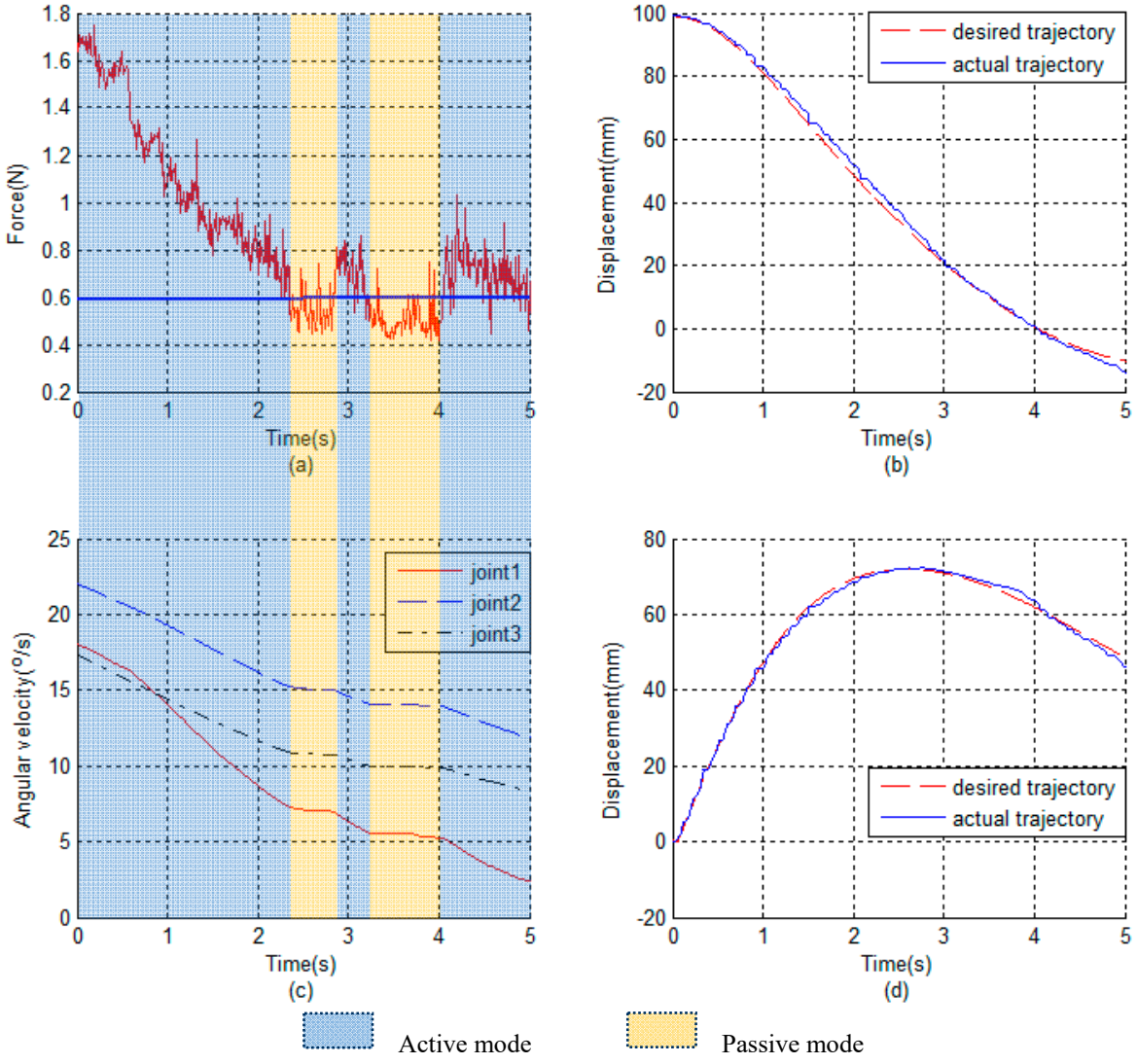

Figure 11. Active plus passive rehabilitation experiment: (**a**) contact force; (**b**) x_t direction displacement; (**c**) joint angle velocity; (**d**) y_t direction displacement.

6. Conclusions

This paper presents a kind of active and passive rehabilitation control strategy and builds the control system of the hand rehabilitation exoskeleton that can accomplish the control strategy.

The hardware system adopts a single chip system based on FPGA to simplify the structure of the hardware circuit and the control system effectively. The Nios II embedded in μC/OS-II core is adopted as a core processor to allow multitasking parallel processing in the control system. Software interactive system adopts open Android as the rehabilitation software's development environment to meet design requirements of the hand rehabilitation exoskeleton, such as portability and handleability. The hand model built in the virtual environment can be driven by the data collected by the underlying control system, that is, synchronizing the movement of the human hand, which can improve the patient's active participation. The active plus passive rehabilitation control strategy is built. Two basic rehabilitation modes can switch actively via fingertip force sensor. The relevant experiment setup is established. Experiments on passive rehabilitation mode, active rehabilitation mod, and active plus passive rehabilitation control are performed, which verifies the feasibility of the control strategy.

In the future, the impedance control system will be improved to be more adaptive with the patients' intention in real time. Moreover, long-term experiments on post-stroke patients will be conducted to testify the efficiency of the whole system in clinics.

Author Contributions: Conceptualization, F.Z.; methodology, F.Z. and L.L.; software, L.Y.; validation, F.Z., L.L., L.Y. and Y.F.; formal analysis, F.Z.; investigation, L.L.; resources, Y.F.; data curation, L.L.; writing—original draft preparation, F.Z.; writing—review and editing, L.L.; visualization, L.L.; supervision, F.Z.; project administration, F.Z.; funding acquisition, F.Z. and Y.F.

Funding: This work was supported in part by the National Natural Science Foundation of China (Grant No. 61673134, 61203347), the Natural Science Foundation of Heilongjiang Province of China (Grant No. LC2017022), and the Postdoctoral Scientific Research Developmental Fund of Heilongjiang Province of China (Grant No. LBH-Q17071).

Conflicts of Interest: The authors declare no conflict of interest.

References

1. Kelly-Hayes, P.M.; Robertson, J.T.; Broderick, J.P.; Duncan, P.W.; Hershey, L.A.; Roth, E.J.; Thies, W.H.; Trombly, C.A. The American Heart Association Stroke Outcome Classification. *Stroke* **1998**, *29*, 1274–1280. [CrossRef] [PubMed]
2. Feigin, V.L. Stroke epidemiology in the developing world. *Lancet* **2005**, *365*, 2160–2161. [CrossRef]
3. French, B.; Thomas, L.H.; Leathley, M.J.; Sutton, C.J.; McAdam, J.; Forster, A.; Langhorne, P.; Price, C.I.M.; Walker, A.; Watkins, C.L. Repetitive Task Training for Improving Functional Ability After Stroke. *Stroke* **2009**, *40*, e98–e99. [CrossRef]
4. Krebs, H.I.; Hogan, N.; Aisen, M.L.; Volpe, B.T. Robot-Aided Neurorehabilitation. *IEEE Trans. Rehabil. Eng.* **1998**, *6*, 75–87. [CrossRef] [PubMed]
5. Vanoglio, F.; Bernocchi, P.; Mulè, C.; Garofali, F.; Mora, C.; Taveggia, G.; Scalvini, S.; Luisa, A. Feasibility and efficacy of a robotic device for hand rehabilitation in hemiplegic stroke patients: A randomized pilot controlled study. *Clin. Rehabil.* **2017**, *31*, 351–360. [CrossRef] [PubMed]
6. Cestari, M.; Sanz-Merodio, D.; Arevalo, J.C.; Garcia, E. An Adjustable Compliant Joint for Lower-Limb Exoskeletons. *IEEE-ASME Trans. Mechatron.* **2015**, *20*, 889–898. [CrossRef]
7. Zanotto, D.; Stegall, P.; Agrawal, S.K. Adaptive assist-as-needed controller to improve gait symmetry in robot-assisted gait training. In Proceedings of the IEEE International Conference on Robotics and Automation (ICRA), Hong Kong, China, 31 May–7 June 2014; pp. 724–729.
8. Pietrusinski, M.; Cajigas, I.; Severini, G.; Bonato, P.; Mavroidis, C. Robotic gait rehabilitation trainer. *IEEE-ASME Trans. Mechatron.* **2014**, *19*, 490–499. [CrossRef]
9. Bos, R.A.; Haarman, C.J.W.; Stortelder, T.; Nizamis, K.; Herder, J.L.; Stienen, A.H.A.; Plettenburg, D.H. A structured overview of trends and technologies used in dynamic hand orthoses. *J. NeuroEng. Rehabil.* **2016**, *13*, 62. [CrossRef]
10. Balasubramanian, S.; Klein, J.; Burdet, E. Robot-assisted rehabilitation of hand function. *Curr. Opin. Neurol.* **2010**, *23*, 661–670. [CrossRef]
11. Ueki, S.; Kawasaki, H.; Ito, S.; Nishimoto, Y.; Abe, M.; Aoki, T.; Ishigure, Y.; Ojika, T. Development of a hand-assist robot with multi-degrees-of-freedom for rehabilitation therapy. *IEEE-ASME Trans. Mechatron.* **2012**, *17*, 136–146. [CrossRef]

12. Fang, H.; Xie, Z.; Liu, H. An exoskeleton master hand for controlling DLR/HIT hand. In Proceedings of the IEEE/RSJ International Conference on Intelligent Robots and Systems (IROS), St. Louis, MO, USA, 10–15 October 2009; pp. 3703–3708.
13. Nakagawara, S.; Kajimoto, H.; Kawakami, N.; Tachi, S.; Kawabuchi, I. An encounter-type multi-fingered master hand using circuitous joints. In Proceedings of the IEEE International Conference on Robotics and Automation (ICRA), Barcelona, Spain, 18–22 April 2005; pp. 2667–2672.
14. Bouzit, M.; Burdea, G.; Popescu, G.; Boian, R. The Rutgers Master II-new design force-feedback glove. *IEEE-ASME Trans. Mechatron.* **2002**, *7*, 256–263. [CrossRef]
15. Wege, A.; Kondak, K.; Hommel, G. Mechanical design and motion control of a hand exoskeleton for rehabilitation. In Proceedings of the IEEE International Conference Mechatronics and Automation, Niagara Falls, ON, Canada, 29 July–1 August 2005; pp. 155–159.
16. Worsnopp, T.; Peshkin, M.; Colgate, J.; Kamper, D. An actuated finger exoskeleton for hand rehabilitation following stroke. In Proceedings of the 2007 IEEE 10th International Conference on Rehabilitation Robotics, Noordwijk, The Netherlands, 13–15 June 2007; pp. 896–901.
17. Shi, Z.; Li, Y.; Liu, G. Adaptive torque estimation of robot joint with harmonic drive transmission. *Mech. Syst. Signal Proc.* **2017**, *96*, 1–15. [CrossRef]
18. Do, T.N.; Tjahjowidodo, T.; Lau, M.W.S.; Phee, S.J. Position control of asymmetric nonlinearities for a cable-conduit mechanism. *IEEE Trans. Autom. Sci. Eng.* **2017**, *14*, 1515–1523. [CrossRef]
19. Li, J.; Wang, S.; Wang, J.; Zheng, R.; Zhang, Y.; Chen, Z. Development of a hand exoskeleton system for index finger rehabilitation. *Chin. J. Mech. Eng.* **2012**, *25*, 223–233. [CrossRef]
20. Heo, P.; Gu, G.; Lee, S.-J.; Rhee, K.; Kim, J. Current hand exoskeleton technologies for rehabilitation and assistive engineering. *Int. J. Precis. Eng. Manuf.* **2012**, *13*, 807–824. [CrossRef]
21. Kim, S.; Lee, J.; Bae, J. Analysis of finger muscular forces using a wearable hand exoskeleton system. *J. Bionic Eng.* **2017**, *14*, 680–691. [CrossRef]
22. Smyrnaiou, G.P.; Papoutsidakis, M.; Xatzopoulos, A.; Tseles, D. Control of SIMO Systems in Simulation: The Challenge of the Multiple Axes Actuating Pneumatic Arm. *Int. J. Comput. Appl.* **2017**, *975*, 8887.
23. Ghassemi, M.; Ranganathan, R.; Barry, A.; Triandafilou, K.; Kamper, D. Introduction of an emg-controlled game to facilitate hand rehabilitation after stroke. In *Converging Clinical and Engineering Research on Neurorehabilitation II*; Springer: Cham, Switzerland, 2017; pp. 451–455.
24. Fu, Y.; Wang, P.; Wang, S.; Liu, H.; Zhang, F. Design and development of a portable exoskeleton based CPM machine for rehabilitation of hand injuries. In Proceedings of the IEEE International Conference on Robotics and Biomimetics (ROBIO), Sanya, China, 15–18 December 2007; pp. 1476–1481.
25. Schabowsky, C.N.; Godfrey, S.B.; Holley, R.J.; Lum, P.S. Development and pilot testing of HEXORR: hand EXOskeleton rehabilitation robot. *J. Neuroeng. Rehabil.* **2010**, *7*, 1–16. [CrossRef]
26. Fischer, H.C.; Stubblefield, K.; Kline, T.; Luo, X.; Kenyon, R.V.; Kamper, D.G. Hand rehabilitation following stroke: a pilot study of assisted finger extension training in a virtual environment. *Top. Stroke Rehabil.* **2007**, *14*, 1–12. [CrossRef]
27. Adissi, M.O.; Lima Filho, A.C.; Gomes, R.D.; Silva, D.M.G.B.; Belo, F.A. Implementation and Deployment of an Intelligent Industrial Wireless System for Induction Motor Monitoring. *J. Dyn. Syst. Meas. Control-Trans. ASME.* **2017**, *139*, 124502. [CrossRef]
28. The Hand Mentor Pro™ Encourages Patients to Actively Participate in Their Recovery with Challenging, Enjoyable Interactive Games. Available online: http://www.webcitation.org/78S5aYEDu (accessed on 18 May 2019).
29. Jack, D.; Boian, R.; Merians, A.S.; Tremaine, M.; Burdea, G.C.; Adamovich, S.V.; Recce, M.; Poizner, H. Virtual reality-enhanced stroke rehabilitation. *IEEE Trans. Neural Syst. Rehabil. Eng.* **2001**, *9*, 308–318. [CrossRef] [PubMed]
30. Zhang, F.; Hua, L.; Fu, Y.; Chen, H.; Wang, S. Design and development of a hand exoskeleton for rehabilitation of hand injuries. *Mech. Mach. Theory* **2014**, *73*, 103–116. [CrossRef]
31. Winter, D.A. *Biomechanics and Motor Control of Human Movement*; Wiley: Hoboken, NJ, USA, 2009; pp. 85–87.